NJC

PAPER

View Article Online
View Journal | View Issue

Cite this: *New J. Chem.*, 2017, **41**, 5066

Improving the growth of monolayer CVD-graphene over polycrystalline iron sheets

M. P. Lavin-Lopez,[a] M. Fernandez-Diaz,[b] L. Sanchez-Silva,[b] J. L. Valverde[b] and A. Romero[b]

Received 23rd January 2017,
Accepted 9th May 2017

DOI: 10.1039/c7nj00281e

rsc.li/njc

A high quality graphene film, mostly composed of monolayer graphene, was successfully grown on polycrystalline iron foil by the CVD process using methane as the carbonaceous source. The effect of the reaction temperature, the CH_4/H_2 flow rate ratio and the total flow of gases (CH_4/H_2) on the formation of graphene during the reaction step at different reaction times was investigated. Optical microscopy and Raman spectroscopy were used as characterization techniques. A homemade Excel-VBA application was designed in order to determine the percentage of the different types of graphene (monolayer, bilayer, few-layer and multilayer) deposited on the metal foil, thus a quantitative quality value was computed. A graphene film deposited under the optimal experimental conditions showed a high percentage of monolayer graphene (62.4% in the sample), a high I_{2D}/I_G ratio (~2.9), a low I_D/I_G ratio (~0.026) and a narrow FWHM of the 2D peak (~22 cm^{-1}). The optimal synthesis conditions were found to be: 1025 °C, CH_4/H_2 = 0.25 v/v, total flow (CH_4 + H_2) = 80 N ml min^{-1} and reaction time = 7 min.

Introduction

Graphene, the most recently discovered carbon allotrope, is a two dimensional (2D) material with a hexagonal lattice structure, composed of a single layer of sp^2-bonded carbon atoms.[1,2] Although graphene has been known since the 1930s, it was not until the year 2004, that Konstantin Novoselov and Andre Geim succeeded in isolating only one atom thick graphene by using the Scotch® tape method.[3,4] A consequence of this discovery is that they were awarded with the Physics Nobel Prize in 2010.[5] Two different strategies can be followed to synthesize graphene which are named as top down and bottom up.[6] Among the bottom up strategy procedures, chemical vapor deposition stands out because it is an inexpensive, quickly and easily scalable method to synthesize large area graphene over transition metals.[7,8] CVD-graphene growth involves the thermal decomposition of a hydrocarbon source (methane, ethylene, acetylene, benzene,...) over a heated substrate.[9] Normally, transition metals such as Ni,[10,11] Pd,[12] Ru,[13] Ir,[14] Cu[15,16] or Fe[17] have been used as catalysts. In a CVD process, the metallic substrates not only act as the catalyst but also determine the growth mechanism. In the case of low carbon solubility metals, such as copper, carbon atoms experience a nucleation and expansion around the nucleus forming graphene domains through hydrocarbon decomposition, catalyzed by the high temperature substrate. The growth process finishes when the substrate is fully covered by graphene layers. This growth mechanism is normally called self-limited surface deposition.[8,18] On the other hand, the growth process when high carbon solubility metals, such as nickel or iron, are used involves the diffusion of carbon atoms into the metal substrate. As the substrate is cooled down, the dissolved carbon segregates to the metal surface forming graphene sheets.[11,18,19] The high quality synthesis of CVD-graphene depends not only on the metallic catalyst but also on the different synthesis conditions.[2] It is most well-known that among all the transition metals, iron has not attracted attention in graphene synthesis in spite of its binary phase diagram and has been used as a catalyst in other CVD synthesis processes, such as that of carbon nanotubes.[20] Iron is cheaper, easier to purchase and easier to etch than other transition metals, which are significant advantages for graphene synthesis. However, few researchers have considered this metal for the synthesis of this carbon material. For example, An *et al.*[17] obtained single to few-layer graphene sheets by partially covering the iron at short exposure times by using acetylene as the carbonaceous source. To achieve continuous graphene layers, large exposure times (15–30 min) are required. Xue *et al.*[21] obtained large area, few-layer high quality graphene over Fe using methane as the carbonaceous source. Some authors[11,15] have reported the relevance of specific variables that can affect the quality of graphene produced. Temperature can be considered as a key factor during CVD-graphene synthesis. Other parameters such as gas flow or exposure time may affect the graphene deposition over the metal substrate.[2] Lavin-Lopez *et al.*[11,15,22]

[a] *Graphenano S.L., Calle Pablo Casals 13, 30510, Yecla, Murcia, Spain. E-mail: pradolavin@graphenano.com*
[b] *University of Castilla-La Mancha, Department of Chemical Engineering, Avenida Camilo Jose Cela 12, 13071, Ciudad Real, Spain*

reported that the control of the exposure to hydrocarbon sources (total flow of gases during the reaction step and the hydrocarbon flow rate ratio), the exposure time and the reaction temperature led to the formation of high quality graphene layers deposited on polycrystalline copper and nickel.

The aim of this work was to optimize the synthesis of atmospheric pressure CVD-graphene over polycrystalline iron foil. Polycrystalline iron has the main advantage of being a cheap material. Thus, the synthesis cost could be considerably reduced in comparison to that of other transition metals commonly used (Ni or Cu). Nitrogen and hydrogen were used as carrier gases and methane was chosen as the carbonaceous source. The main variables that might affect the graphene growth (reaction temperature, the CH_4/H_2 flow rate ratio and total flow during the reaction step at different reaction times) were studied in detail in order to increase the percentage of monolayer graphene deposited over the iron substrate.

Experimental

Materials

Methane (99.5%), hydrogen (99.999%) and nitrogen (99.999%) were purchased from Praxair. 25 μm thick polycrystalline iron foil with a purity of 99.99% was purchased from Goodfellow.

Method

Graphene samples were grown in an atmospheric pressure CVD system composed of a 40-inch quartz tube encased into a furnace (Fig. 1a). Graphene samples were deposited over 25 μm thick polycrystalline iron sheets, which were used as catalysts. The furnace was heated to the reduction temperature (900 °C) under 400 sccm flow of N_2 and 100 sccm flow of H_2. The furnace was maintained at this temperature for 45 minutes to complete the reduction step and allow the annealing of the metal sheet. After that, the selected reaction temperature (900–1050 °C) was reached and 30 sccm of CH_4 flow was introduced into the furnace while N_2 flow was turned off during the reaction time (5–15 min). Finally, the system was cooled down by flowing 400 sccm of N_2 (Fig. 1b).

Graphene characterization techniques

Raman spectroscopy. A SENTERRA Raman spectrometer, with 600 lines per mm grating and 532 nm laser wavelength at a very low laser power level (<1 mW) to avoid any heating effect, was used to characterize the graphene obtained over the polycrystalline iron.

Optical microscopy. A SENTERRA X50 microscope equipped with the OPUS software was used to analyze the graphene synthesized. Around fifty optical microscopy images (OMIs) were analyzed per sample but only six were considered as representative ones. In each optical microscopy image, four different colors could be observed, corresponding each one to one type of graphene (monolayer, bilayer, few-layer and multilayer). By using Raman spectroscopy, it was checked that lighter colors correspond to a lower number of graphene layers (white areas correspond to monolayer graphene and yellow areas to bilayer graphene) whereas darker colors correspond to a higher number of graphene layers (dark orange corresponds to multilayer graphene and the lighter one to few-layer graphene).

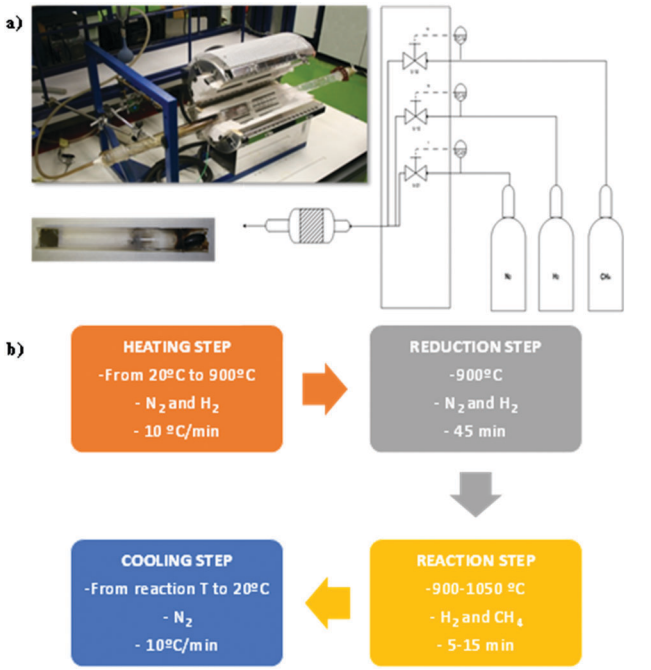

Fig. 1 (a) CVD-graphene synthesis experimental installation and (b) synthesis procedure for CVD-graphene synthesis.

SEM and EDX. The morphology of the samples was observed using a scanning electron microscope (SEM) (Phenom ProX). Elemental analysis was carried out using the EDX software of SEM equipment. In order to obtain a representative analysis of the sample, 200 elemental analyses of each graphene sample were performed, their median value is shown in this manuscript.

Excel-VBA application: determination of a quality value related to the thickness of the samples

A homemade Excel-VBA application was programmed to determine a graphene quality value, which is closely related to the thickness of the number of graphene layers. The smaller the graphene thickness, the lower the amount of graphene covering the iron foil and, thus, the higher the quality value obtained for the graphene sample.

First of all, Excel-VBA application analyzes the optical microscopy images of graphene by checking the different colors presented on it, which are related to the different types of graphene (multilayer, few-layer, bilayer or monolayer) as corroborated using Raman spectroscopy. In addition, the application calculates the percentage of each type of graphene covering the sample corresponding to colors present in the optical microscopy images. Thus, quality values of 1, 10, 100 and 1000 were assigned to 100% of the iron foil covered with multilayer, few-layer, bilayer and monolayer graphene, respectively. The quality value of the graphene sample was calculated as an average of the percentage obtained for each type of graphene[11,15,22] (Fig. 2). In order to check how representative of the entire sample is the quality value, the error bars have been included.

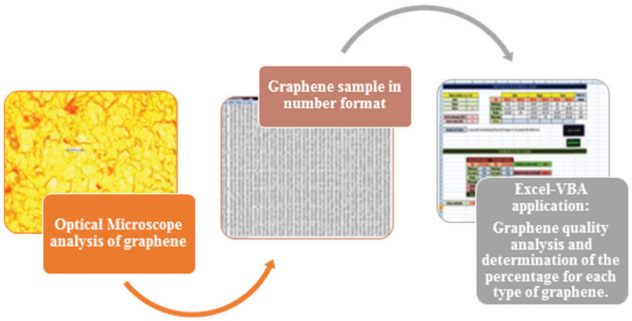

Fig. 2 Excel-VBA application to determine the percentage of each type of graphene and the graphene quality value.

Results and discussion

Influence of the reaction temperature

In order to analyze the influence of the reaction temperature on the number of graphene layers in the products (through the determination of a quality value), different experiments were performed between 900 and 1050 °C. It has been demonstrated that the reaction temperature plays an important role in the graphene characteristics.[11,15,23] Xu *et al.*[21] reported that a suitable temperature influenced over the graphene crystallinity and, consequently, over its thickness.

A maximum quality value of 354.2 was obtained for the sample synthesized at 1025 °C. At this temperature, 30.77% of the iron foil was covered with monolayer graphene and 44.8% with bilayer graphene. Only 7.2% of the iron sheet presented multilayer graphene over it.

Around fifty optical microscopy images taken in different areas of each product obtained at each temperature were used for a representative analysis. Four different colors could be distinguished in these optical microscopy images. Raman spectroscopy demonstrated that each color corresponded to one type of graphene (see Fig. 3 where it is possible to observe the Raman spectrum of a parent iron foil and that of a random graphene sample).

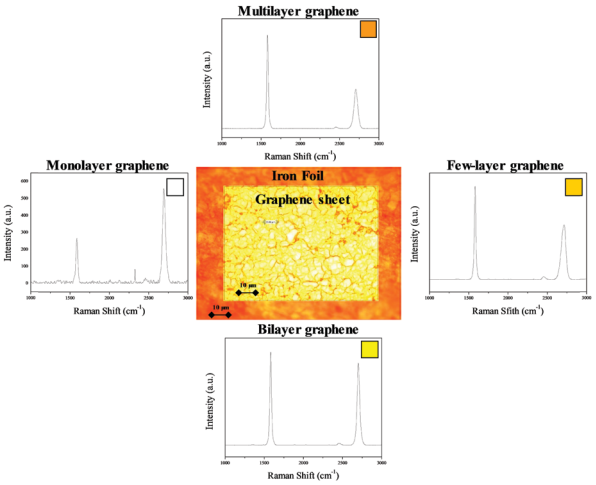

Fig. 3 Raman spectra corresponding to the different zones observed in optical microscopy images.

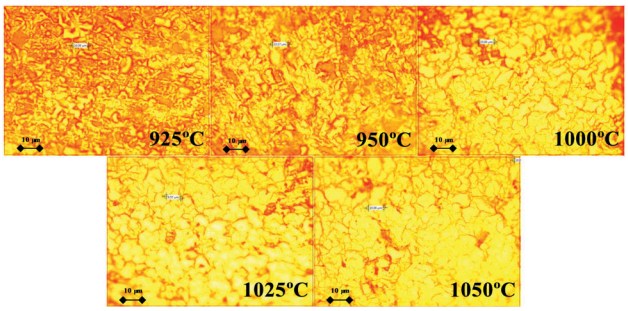

Fig. 4 Influence of the reaction temperature. Optical microscopy images at different reaction temperatures. (Synthesis conditions: 925–1050 °C, CH_4/H_2 = 0.30 v/v, 130 N ml min^{-1}, 10 minutes of reaction time.)

Thus, darker orange colors, mostly visible at the grain boundaries, correspond to multilayer graphene; lighter orange colors are assigned to few-layer graphene; yellow areas correspond to bilayer graphene and, finally, white and lighter areas are assigned to monolayer graphene.[11,15] Optical microscopy images generated using a Raman spectrometer were analyzed by using a homemade Excel-VBA application, thus, the corresponding quality value and the percentage of each type of graphene were evaluated for all the samples prepared at different temperatures.

Fig. 4 shows an optical microscopy image for the sample obtained at different reaction temperatures. As observed, orange colors were more intense for lower reaction temperatures (925–950 °C). Conversely, the higher the reaction temperature, the lower the intensity of the colors was. Below 925 °C, it was not possible to observe continuous graphene growth over the polycrystalline iron foil.

The analysis of the images generated using an optical microscope of the Raman spectrometer by the Excel-VBA application allowed us to determine the percentage of each type of graphene deposited over the iron foil at different temperatures (Table 1). As is observed, the percentage of monolayer and bilayer graphene increased with the reaction temperature until 1025 °C was reached.

Fig. 5 shows the variation of the quality value as a function of the reaction temperature. Polycrystalline metals have irregular surfaces with a high amount of grain boundaries, which facilitate the formation of more layered graphene because impurities present in these metals have a tendency to segregate at these positions.[24] Thus, at low reaction temperatures (925–1000 °C), most of the dissolved carbon atoms were deposited over these grain boundaries, favoring the formation of more layered graphene and, consequently, decreasing the quality value.

Table 1 Influence of the reaction temperature. Average values of each type of graphene obtained from the representative optical microscopy images. (Synthesis conditions: 925–1050 °C, CH_4/H_2 = 0.30 v/v, 130 N ml min^{-1}, 10 minutes of reaction time)

T (°C)	Monolayer (%)	Bilayer (%)	Few-layer (%)	Multilayer (%)
925	2.6	23.2	31.3	43
950	3.8	28.2	32.9	35.1
1000	14.1	42.3	26.0	17.6
1025	*31.5*	*44.1*	*17.1*	*7.4*
1050	21.8	50.3	20	7.9

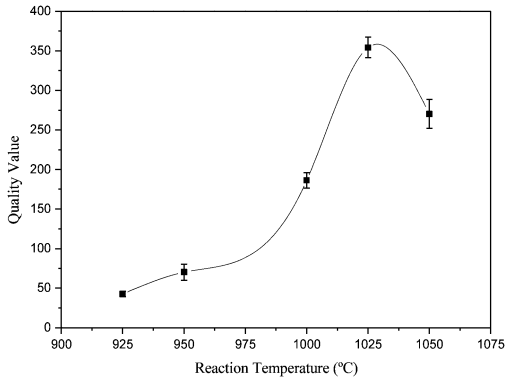

Fig. 5 Influence of the reaction temperature. Quality value *vs.* reaction temperature.

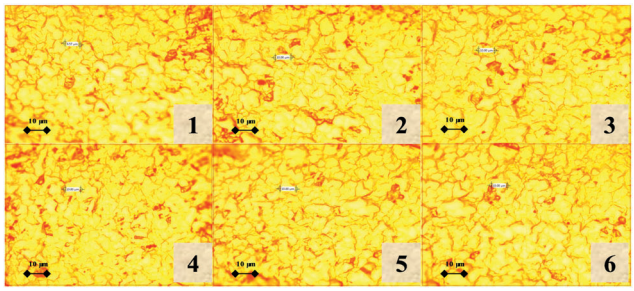

Fig. 6 Optical microscopy images taken in different areas of the sample synthesized at 1025 °C. (Synthesis conditions: 1025 °C, CH_4/H_2 = 0.30 v/v, 130 N ml min^{-1}, 10 minutes of reaction time.)

Table 2 Optimum reaction temperature. Quality and percentage of each type of graphene deposited over the optimum sample. (Synthesis conditions: 1025 °C, CH_4/H_2 = 0.30 v/v, 130 N ml min^{-1}, 10 minutes of reaction time)

OMI	Monolayer (%)	Bilayer (%)	Few-layer (%)	Multilayer (%)	Quality value
1	28.34	46.94	18.29	6.43	332.3
2	31.45	43.41	16.49	8.65	359.7
3	30.04	47.57	16.83	5.56	349.7
4	29.99	44.22	16.36	9.43	345.8
5	30.89	43.04	18.68	7.38	353.9
6	33.89	43.30	16.94	5.87	384.0
Average	*30.77*	*44.75*	*17.27*	*7.21*	*354.2*

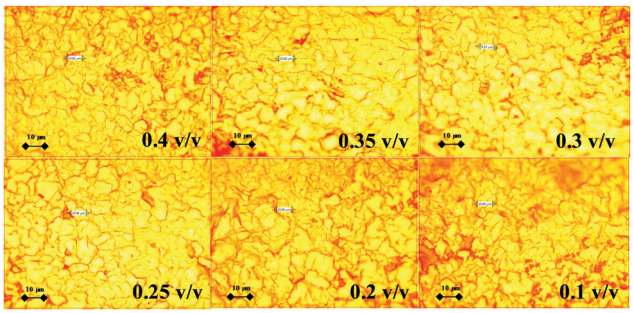

Fig. 7 Influence of the CH_4/H_2 flow rate ratio. Optical microscopy images obtained at different CH_4/H_2 flow rate ratios. (Synthesis conditions: 1025 °C, CH_4/H_2 = 0.1–0.4 v/v, 130 N ml min^{-1}, 10 minutes of reaction time.)

However, at high temperatures, the dissolution of grain boundaries of the metal sheet on iron foil and the high solubility of carbon oil promote the formation of less layered graphene,[25,26] leading to an increase in the graphene quality. However, an excessively high temperature (1050 °C) could cause an excessive solubility of the carbon atoms, leading to the formation of graphite flakes and, consequently, decreasing the quality value of the samples. Hence, the growth of monolayer graphene is less favored.[17] 1025 °C was considered to be the optimal reaction temperature at which there is a balance between the synthesis of high quality graphene, a proper carbon dissolution and a low amount of grain boundaries. As it will be shown below, at this temperature the quality was maximum (354.2).

Fig. 6 shows the optical microscopy images selected (among more than 50 images) for the sample synthesized at 1025 °C (optimum reaction temperature) whereas Table 2 lists the corresponding quality value and the percentage of each type of graphene obtained. At this temperature, 30.8% of the sample was covered with monolayer graphene and the 44.8% with bilayer graphene.

Influence of the CH_4/H_2 flow rate ratio

The influence of the CH_4/H_2 flow rate ratio was ranged between 0.4 and 0.1 v/v. The other synthesis parameters which influence in this study were maintained constant (1025 °C reaction temperature, 130 N ml min^{-1} of total flow rate ratio and 10 minutes of reaction time). Methane flow has been revealed as an important factor during graphene growth.[11,15,22] Xue *et al.*[21] reported that a decrease in the methane flow from 300 to 180 sccm allowed us to obtain bilayer graphene instead of multilayer one. This fact was due to the smaller amount of carbon that was dissolved and segregated into and from the catalyst, respectively.

Fig. 7 shows a representative optical microscopy image of the samples obtained at each of the CH_4/H_2 flow rate ratio studied.

Again, around fifty optical microscopy images taken in different areas of each product obtained at each CH_4/H_2 flow rate ratio were used to obtain a representative value of the quality and the percentage of each type of graphene deposited over the polycrystalline iron foil (Table 3). Note that as the CH_4/H_2 flow rate ratio decreased up to a value of 0.25 v/v, the percentage of monolayer graphene on the iron foil grew up.

Fig. 8 shows the variation of the quality value as a function of the CH_4/H_2 flow rate ratio. The higher the CH_4/H_2 flow rate ratio, the higher the amount of CH_4 flowed into the system and, thus, the more the carbon atoms dissolved that would be deposited over the metal foil. Some researchers have reported that with iron foil and low methane flow rates, the formation of few layered graphene is favored probably due to the smaller amount of carbon atoms dissolved and segregated from the metal foil.[2,21] For the highest CH_4/H_2 flow rate ratio (0.4 v/v), an excess of carbon atoms would be deposited over the iron sheet leading to the formation of more layered graphene, thus obtaining a quality value of 159.6. This quality value increased by decreasing the CH_4/H_2 flow rate ratio until a maximum quality value (356.9) was reached for a CH_4/H_2 flow rate ratio of 0.25 v/v. The quality value drastically decreased when the

Table 3 Influence of the CH_4/H_2 flow rate ratio. Average values of each type of graphene obtained from the representative optical microscopy images

CH_4/H_2 flow rate ratio	Monolayer (%)	Bilayer (%)	Few-layer (%)	Multilayer (%)
0.4	11.05	46.06	29.53	13.35
0.35	23.77	45.14	20.66	10.44
0.3	29.55	45.58	17.72	7.15
0.25	*30.77*	*44.75*	*17.27*	*7.21*
0.2	8.09	46.19	31.20	14.51
0.1	5.44	40.37	34.58	19.60

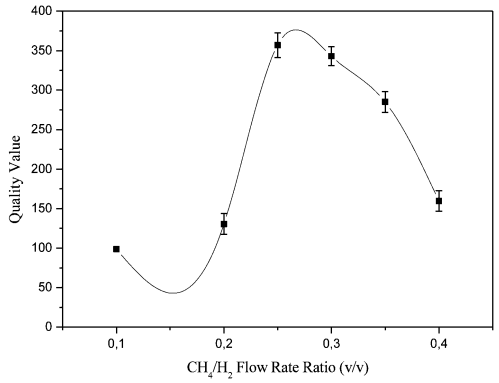

Fig. 8 Influence of the CH_4/H_2 flow rate ratio. Quality value *vs.* CH_4/H_2 flow rate ratio.

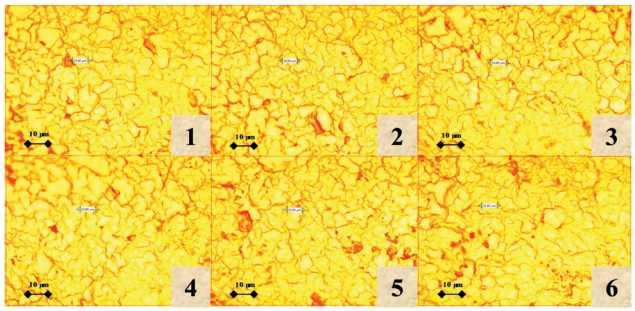

Fig. 9 Optical microscopy images taken in different areas of the sample synthesized at 0.25 v/v. (Synthesis conditions: 1025 °C, CH_4/H_2 = 0.25 v/v, 130 N ml min^{-1}, 10 minutes of reaction time.)

CH_4/H_2 flow rate ratio was also decreased, thus leading to the production of non-homogeneous graphene. Fig. 9 shows the optical microscopy images (among more than 50 images) corresponding to the sample synthesized using a CH_4/H_2 flow rate ratio of 0.25 v/v, which was considered as the optimum value. The corresponding percentage of each type of graphene and its quality value is listed in Table 4.

As observed, the CH_4/H_2 flow rate ratio has an influence on the percentage of monolayer graphene deposited over the polycrystalline iron foil.

Influence of the total flow of gases (CH_4 + H_2) during the reaction step at different reaction times

The optimization of the value of the total flow of gases during the reaction step, at different reaction times (15–5 min), has been performed in the range from 130 and 60 N ml min^{-1}. It has been reported that the influence of the total flow during the reaction step is closely related to that of the reaction time. Longer exposure times to the reaction gases are required for their low total flow, because the amount of carbonaceous source flowing during the reaction step is low and, consequently, longer times are also required to obtain an homogeneous graphene layer.[17,22,27]

Table 4 Optimum CH_4/H_2 flow rate ratio. Quality and percentage of each type of graphene deposited over the optimum sample. (Synthesis conditions: 1025 °C, CH_4/H_2 = 0.25 v/v, 130 N ml min^{-1}, 10 minutes of reaction time)

OMI	Monolayer (%)	Bilayer (%)	Few-layer (%)	Multilayer (%)	Quality value
1	33.46	41.80	17.30	7.45	378.2
2	34.28	41.46	17.38	6.88	386.1
3	31.13	41.84	17.57	9.46	355.0
4	28.95	43.90	18.62	8.52	335.4
5	30.27	43.38	18.50	7.84	348.0
6	29.34	43.17	18.98	8.51	338.5
Average	*31.24*	*42.60*	*18.1*	*8.11*	*356.9*

Fig. 10 shows the representative optical microscopy images corresponding to each sample synthesized using different total flows (130–60 N ml min^{-1}) and exposure times (5–15 minutes). The corresponding percentages of each type of graphene deposited over the iron foil, determined by the homemade Excel-VBA application, are listed in Table 5.

Different authors have reported that a balance between the value of reaction time and that of the total flow of gases is needed to promote the growth of monolayer graphene over metal foil since excessively high reaction times can result in the formation of more layered graphene.[27,28] As expected, the lower

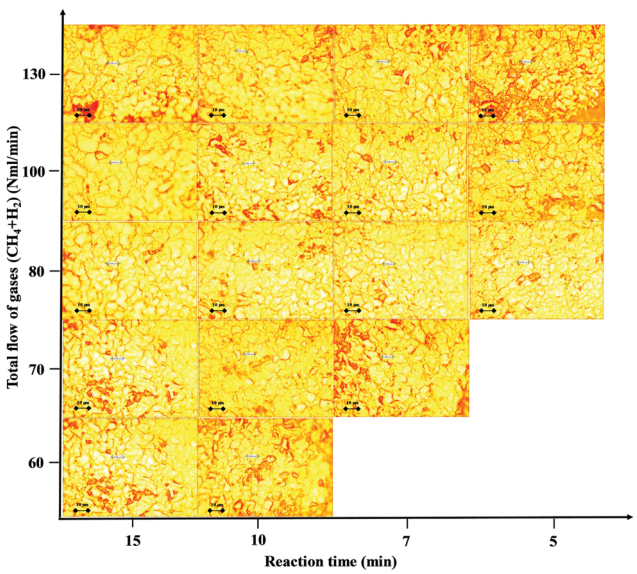

Fig. 10 Influence of the total flow of gases (CH_4 + H_2) during the reaction step at different reaction times. Optical microscopy images. (Synthesis conditions: 1025 °C, CH_4/H_2 = 0.25 v/v, 130–60 N ml min^{-1}, 15–5 minutes of reaction time.)

Table 5 Influence of the total flow of gases (CH_4 + H_2) during the reaction step at different reaction times. Average values of each type of graphene obtained from the representative optical microscopy images. (Synthesis conditions: 1025 °C, CH_4/H_2 = 0.25 v/v, 130–60 N ml min^{-1}, 15–5 minutes of reaction time)

Total flow of gases (N ml min^{-1})	Reaction time (min)	Monolayer (%)	Bilayer (%)	Few-layer (%)	Multilayer (%)
130	15	31.41	37.51	18.71	12.38
	10	31.24	45.59	18.05	8.11
	7	*34.81*	*38.49*	*17.30*	*9.40*
	5	17.56	32.78	23.59	26.07
100	15	36.78	44.91	13.26	5.04
	10	42.40	33.76	14.28	9.55
	7	*51.39*	*29.88*	*11.70*	*7.02*
	5	31.02	34.91	19.37	14.71
80	15	51.78	31.38	11.59	5.24
	10	54.56	28.13	11.17	6.14
	7	*62.4*	*24.57*	*8.75*	*4.29*
	5	57.97	26.31	9.91	5.81
70	*15*	*51.71*	*27.58*	*10.39*	*8.54*
	10	34.78	39.49	17.18	8.53
	7	31.97	30.50	18.00	19.52
60	*15*	*42.26*	*32.59*	*12.25*	*5.89*
	10	31.86	32.33	19.18	16.63

the total flow of gases, the longer the reaction times are required to obtain less layered structures (corresponding to optical microscopy images where light colors predominate in a uniform way). At low total flow of gases (60–70 N ml min^{-1}) and times less than 10 min, the graphene growth was not favored as a result of not having carbon atoms enough flowing through the reaction system to achieve a uniform deposition of graphene over the polycrystalline iron foil. Moreover, at low total flows (60 and 70 N ml min^{-1}), zones presenting free-graphene islands were observed. On the other hand, the higher the total flow (130 and 100 N ml min^{-1}) was, the darker the colors presented in the optical microscopy images were observed, thus observing orange (in different color tonalities) zones that correspond to multilayer graphene. For the intermediate value of the total flow (80 N ml min^{-1}), clearer colors were observed in the microscopy images (lower thickness value) (Table 5).

Fig. 11 shows the quality value *versus* the total flow of gases (CH_4 + H_2) at different reaction times. A maximum of quality value was obtained for the sample synthesized using a total flow of 80 N ml min^{-1} and 7 minutes of reaction time. Fig. 12 shows the more representative optical microscopy images corresponding to this optimal sample whereas Table 6 lists the quality and the percentage of each type of graphene deposited on it (Table 6). As observed, this optimal sample presented a value of the percentage of monolayer graphene deposited over the metal foil close to 62.5%.

As observed, the growth of the monolayer graphene over the polycrystalline iron foil clearly depends on the total flow of gases passing through it and the exposure time to such gases.

Finally, Fig. 13 shows the Raman spectroscopy results and the 2D peak deconvolution corresponding to the different

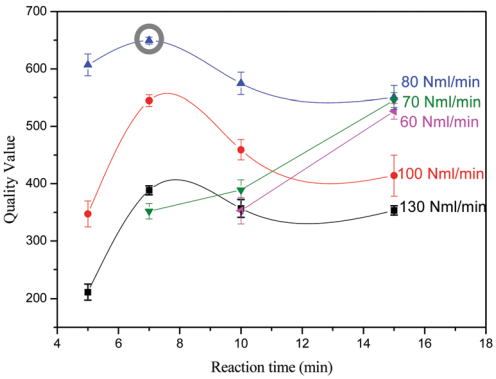

Fig. 11 Influence of the total flow of gases (CH_4 + H_2) during the reaction step at different reaction times. Quality value *vs.* reaction time at the different total flow of gases (CH_4 + H_2).

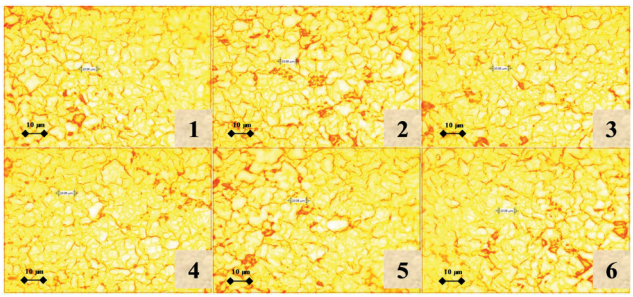

Fig. 12 Optical microscopy images taken in different areas of the sample synthesized at 80 N ml min^{-1} and 1 minute of reaction time. (Synthesis conditions: 1025 °C, CH_4/H_2 = 0.25 v/v, 80 N ml min^{-1}, 7 minutes of reaction time.)

Table 6 Optimum total flow of gases (CH_4 + H_2) during the reaction step at different reaction times. Quality and percentage of each type of graphene deposited over the optimum sample. (Synthesis conditions: 1025 °C, CH_4/H_2 = 0.25 v/v, 80 N ml min^{-1}, 7 minutes of reaction time)

OMI	Monolayer graphene (%)	Bilayer graphene (%)	Few-layer graphene (%)	Multilayer graphene (%)	Quality value
1	62.45	25.26	8.71	3.58	650.7
2	61.86	22.31	9.94	5.89	642.0
3	61.48	25.95	8.30	4.27	641.6
4	63.40	25.58	7.88	3.14	660.4
5	61.90	24.14	9.50	4.47	644.1
6	63.31	24.16	8.15	4.37	658.1
Average	*62.4*	*24.57*	*8.75*	*4.29*	649.5

graphene types presented in the optimum sample. Raman spectroscopy parameters (I_D/I_G, I_{2D}/I_G, FWHM and 2D peak position) agree with those reported in the literature.[16,29–35]

All types of graphene showed insignificant I_D/I_G ratio values indicating that they are defect-free. The I_{2D}/I_G ratio increased when the number of graphene layers decreased, achieving for monolayer graphene the highest value (2.86). The opposite effect was observed for the FWHM parameters. They decreased with decreasing graphene layers, obtaining for monolayer graphene the lowest value (22 cm^{-1}). The 2D peak position

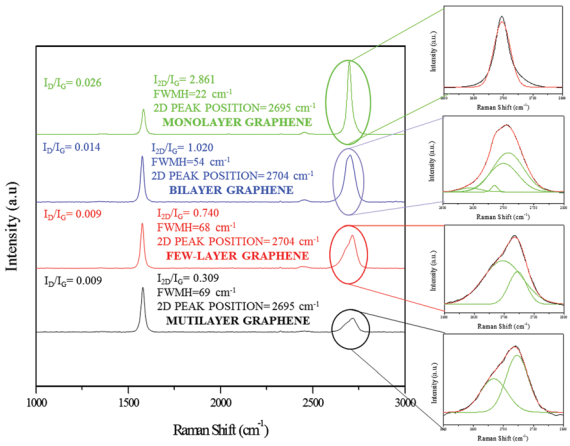

Fig. 13 Raman spectroscopy results corresponding to the optimum sample. (Synthesis conditions: 1025 °C, CH_4/H_2 = 0.25 v/v, 80 N ml min^{-1}, 7 minutes of reaction time.)

was located at around 2700 cm^{-1} for all graphene types, which is a characteristic value of this material.[11,15,22,36]

Finally, 2D peak deconvolution confirmed the typology of the graphene present in the sample.[37] According to the literature, the 2D peak was deconvoluted in a single Lorentzian peak for monolayer graphene; this peak was split into four different peaks in bilayer graphene.[38] Finally, 2D peaks corresponding to few-layer and multilayer graphene were deconvoluted into two peaks.[11]

Fig. 14 shows SEM analysis corresponding to the optimum sample (1025 °C, CH_4/H_2 = 0.25 v/v, 80 N ml min^{-1}, 7 minutes of reaction time). Different scales (10 μm, 5 μm and 1 μm) can be observed in SEM images and the contrast between more and less layered graphene can be observed properly. In all SEM images it is possible to observe the structure of the graphene

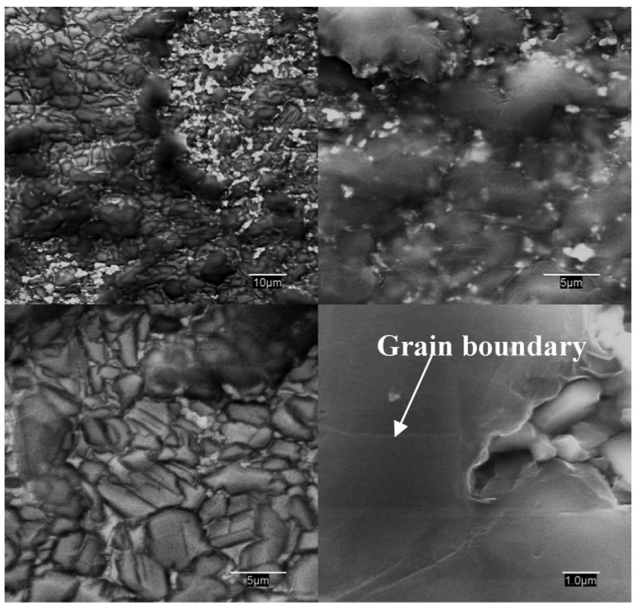

Fig. 14 SEM images corresponding to the optimum CVD-graphene sample. (Synthesis conditions: 1025 °C, CH_4/H_2 = 0.25 v/v, 80 N ml min^{-1}, 7 minutes of reaction time.)

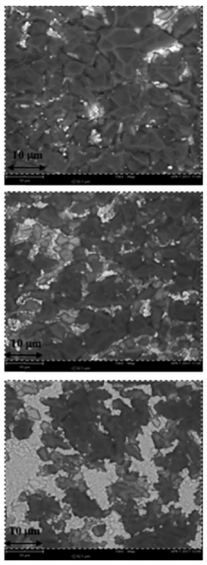

OPTIMUM TEMPERATURE		
Element Symbol	Weight Concentration	Quality Value
C	87.2	354.2
Fe	12.84	

OPTIMUM CH_4/H_2 FLOW RATE RATIO		
Element Symbol	Weight Concentration	Quality Value
C	77.6	356.9
Fe	22.4	

OPTIMUM TOTAL FLOW AND TIME		
Element Symbol	Weight Concentration	Quality Value
C	57.0	649.5
Fe	33.0	

Fig. 15 SEM and EDX analysis of optimum graphene samples.

sample differentiating darker and lighter areas which correspond to more and less layered graphene, respectively. At 1 μm, grain boundaries are clearly visible, demonstrating that metal used as a catalyst is polycrystalline.

In order to corroborate the decrease of graphene layers with the optimization of CVD-graphene synthesis conditions, SEM analysis combined by elemental analysis (EDX) of the optimum samples have been performed (Fig. 15). Results showed that carbon percentage decreased and consequently, iron percentage increased, with the optimization of the synthesis conditions. In this way, 87.2% of carbon was obtained for the optimum temperature sample (1025 °C). At this optimum temperature, a quality value of around 355 was obtained and the predominance of bilayer graphene over the sample was obtained. This fact can be observed in the SEM image, which is covered mostly with black color that corresponds to more layered graphene. The optimization of the CH_4/H_2 flow rate ratio (0.25 v/v) increased the quality value to around 357 which was reflected in the decrease of the carbon percentage to 77.6%. In this sense, it was considered that lower percentage of carbon corresponds to a lower number of graphene layers in the sample. As a consequence, lighter areas were observed in the SEM images. The minimum percentage of carbon (57%) was obtained for the optimum sample (1025 °C, CH_4/H_2 = 0.25 v/v, 80 N ml min^{-1}, 7 minutes of reaction time). Under these reaction conditions, a quality value of around 650 was obtained, with more than 60% of the sample being covered by monolayer graphene which has been related to the increase of lighter areas in the SEM images.

Fig. 16 shows a general comparison of the optimum synthesis conditions of CVD-graphene grown over different polycrystalline transition metal foils. Although nickel required a lower reaction time and reaction temperature to obtain the optimum conditions, its prize is quite higher than that of iron, justifying the use of polycrystalline iron foil on the industrial scale.

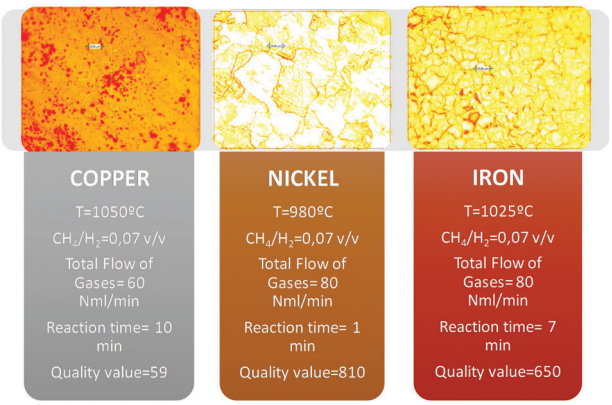

Fig. 16 Comparison between CVD-graphene grown over different transition metals.

Conclusions

In the present work, it has been demonstrated that a high quality graphene film, mostly covered by monolayer graphene, can be successfully grown on polycrystalline iron foil by an atmospheric pressure CVD process using methane as the carbonaceous source. The thickness of the graphene sample (number of layers) can be controlled by tuning the reaction temperature, the CH_4/H_2 flow rate ratio and the total flow of gases ($CH_4 + H_2$) during the reaction step at different reaction times. By means of a process of parameter optimization, a high quality graphene film was achieved, showing a high percentage of monolayer graphene (62.4%), a high I_{2D}/I_G ($\sim$2.9), a low I_D/I_G ratio ($\sim$0.026) and a narrow FWHM of the 2D peak ($\sim$22 cm^{-1}).

The quality of graphene films could be enhanced by increasing the growth temperature and the CH_4/H_2 flow rate ratio up to 1025 °C and 0.25 v/v, respectively. In addition, low values of the total flow ($CH_4 + H_2$) of gases (80 N ml min^{-1}) and short exposure times (7 minutes) were found to be required for obtaining high quality graphene.

These findings could help manufacture high-quality graphene on iron foil for different applications, mainly electronic ones.

Notes and references

1 A. K. Geim and K. S. Novoselov, *Nat. Mater.*, 2007, **6**, 183–191.
2 R. Muñoz and C. Gómez-Aleixandre, *Chem. Vap. Deposition*, 2013, **19**, 297–322.
3 M. I. Katsnelson, *Mater. Today*, 2007, **10**, 20–27.
4 E. P. Randviir, D. A. C. Brownson and C. E. Banks, *Mater. Today*, 2014, **17**, 426–432.
5 Kungliga Vetenskapsakademien - Hem [Internet], http://www.kva.se/en/, Accessed 01-23, 2016.
6 M. P. Lavin-Lopez, J. L. Valverde, L. Sanchez-Silva and A. Romero, *Ind. Eng. Chem. Res.*, 2016, **55**, 845–855.
7 S. Bae, H. Kim, Y. Lee, X. Xu, J. S. Park, Y. Zheng, J. Balakrishnan, T. Lei, H. Ri Kim, Y. I. Song, Y. J. Kim, K. S. Kim, B. Özyilmaz, J. H. Ahn, B. H. Hong and S. Iijima, *Nat. Nanotechnol.*, 2010, **5**, 574–578.
8 L. Huang, Q. H. Chang, G. L. Guo, Y. Liu, Y. Q. Xie, T. Wang, B. Ling and H. F. Yang, *Carbon*, 2012, **50**, 551–556.
9 M. S. A. Bhuyan, M. N. Uddin, M. M. Islam, F. A. Bipasha and S. S. Hossain, *Int. Nano Lett.*, 2016, **6**, 65–83.
10 K. S. Kim, Y. Zhao, H. Jang, S. Y. Lee, J. M. Kim, J. H. Ahn, P. Kim, J. Y. Choi and B. H. Hong, *Nature*, 2009, **457**, 706–710.
11 M. P. Lavin-Lopez, J. L. Valverde, M. I. Ruiz-Enrique, L. Sanchez-Silva and A. Romero, *New J. Chem.*, 2015, **39**, 4414–4423.
12 M. Choucair, P. Thordarson and J. A. Stride, *Nat. Nanotechnol.*, 2009, **4**, 30–33.
13 P. W. Sutter, J. I. Flege and E. A. Sutter, *Nat. Mater.*, 2008, **7**, 406–411.
14 J. Coraux, A. T. N'Diaye, C. Busse and T. Michely, *Nano Lett.*, 2008, **8**, 565–570.
15 M. P. Lavin-Lopez, J. L. Valverde, M. C. Cuevas, A. Garrido, L. Sanchez-Silva, P. Martinez and A. Romero-Izquierdo, *Phys. Chem. Chem. Phys.*, 2014, **16**, 2962–2970.
16 A. Reina, X. Jia, J. Ho, D. Nezich, H. Son, V. Bulovic, M. S. Dresselhaus and K. Jing, *Nano Lett.*, 2009, **9**, 30–35.
17 H. An, W. J. Lee and J. Jung, *Curr. Appl. Phys.*, 2011, **11**, S81–S85.
18 X. Chen, L. Zhang and S. Chen, *Synth. Met.*, 2015, **210**(Part A), 95–108.
19 Q. Yu, J. Lian, S. Siriponglert, H. Li, Y. P. Chen and S. S. Pei, *Appl. Phys. Lett.*, 2008, **93**, 113103.
20 K. A. Shah and B. A. Tali, *Mater. Sci. Semicond. Process.*, 2016, **41**, 67–82.
21 Y. Xue, B. Wu, Y. Guo, L. Huang, L. Jiang, J. Chen, D. Geng, Y. Liu, W. Hu and G. Yu, *Nano Res.*, 2011, **4**, 1208–1214.
22 M. P. Lavin-Lopez, J. L. Valverde, L. Sanchez-Silva and A. Romero, *J. Nanomater.*, 2016, **2016**, 9.
23 Y. Shen and A. C. Lua, *Sci. Rep.*, 2013, **3**, 3037.
24 Y. M. Wang, S. Cheng, Q. M. Wei, E. Ma, T. G. Nieh and A. Hamza, *Scr. Mater.*, 2004, **51**, 1023–1028.
25 A. J. Van Bommel, J. E. Crombeen and A. Van Tooren, *Surf. Sci.*, 1975, **48**, 463–472.
26 K. Verguts, B. Vermeulen, N. Vrancken, K. Schouteden, C. Van Haesendonck, C. Huyghebaert, M. Heyns, S. De Gendt and S. Brems, *J. Phys. Chem. C*, 2016, **120**, 297–304.
27 H. Yang, C.-M. Shen, Y. Tian, G.-Q. Wang, S.-X. Lin, Y. Zhang, C.-Z. Gu, J.-J. Li and H.-J. Gao, *Chin. Phys. B*, 2014, **23**, 096803.
28 A. Dathbun and S. Chaisitsak, 8th IEEE International Conference on Nano/Micro Engineered and Molecular Systems (NEMS), 2013, pp. 1018–1021.
29 X. Li, W. Cai, J. An, S. Kim, J. Nah, D. Yang, R. Piner, A. Velamakanni, I. Jung, E. Tutuc, S. K. Banerjee, L. Colombo and R. S. Ruoff, *Science*, 2009, **324**, 1312–1314.
30 J. Y. Hwang, C. C. Kuo, L. C. Chen and K. H. Chen, *Nanotechnology*, 2010, **21**, 315201.
31 C. Mattevi, H. Kim and M. Chhowalla, *J. Mater. Chem.*, 2011, **21**, 3324–3334.

32 G. Ruan, Z. Sun, Z. Peng and J. M. Tour, *ACS Nano*, 2011, **5**, 7601–7607.
33 S. Chen, W. Cai, R. D. Piner, J. W. Suk, Y. Wu, Y. Ren, J. Kang and R. S. Ruoff, *Nano Lett.*, 2011, **11**, 3519–3525.
34 S. Lee, K. Lee and Z. Zhong, *Nano Lett.*, 2010, **10**, 4702–4707.
35 D. Lee, K. Lee, S. Jeong, J. Lee, B. Choi and O. Kim, *Jpn. J. Appl. Phys.*, 2012, **51**, 06FD21.
36 R. J. Nemanich and S. A. Solin, *Phys. Rev. B: Condens. Matter Mater. Phys.*, 1979, **20**, 392–401.
37 A. C. Ferrari, J. C. Meyer, V. Scardaci, C. Casiraghi, M. Lazzeri, F. Mauri, S. Piscanec, D. Jiang, K. S. Novoselov, S. Roth and A. K. Geim, *Phys. Rev. Lett.*, 2006, **97**, 187401.
38 B. Ryan, C. Luiz Gustavo and N. Lukas, *J. Phys.: Condens. Matter*, 2015, **27**, 083002.

